

## Interfacial microstructure of $\text{Al}_4\text{C}_3$ in SiC/Al-Mg composite fabricated by melt spinning technique

Emad M. Ahmed

Material and Corrosion Group, Physics Department, Faculty of Science, Taif University, P.O. Box 888, Taif 21974, (KINGDOM OF SAUDI ARABIA)

Solid State Physics Department, National Research Center, Dokki, Giza 12311, (EGYPT)

E-mail: makboul67@yahoo.com

### ABSTRACT

Al–10 wt.%Mg alloy was reinforced with 2wt.% SiC nanoparticles by vortex techniques then rapidly solidified by melt spinning. Particle interaction with metal-matrix and tensile properties in as-spun condition were studied. The resulting as-spun composite structure was analyzed using DTA, XRD, SEM and EDX. The microstructure showed excellent distribution of Mg, Si and C into Al matrix. In addition, it was proved the formation of  $\text{Al}_4\text{C}_3$  nanosheet of two dimensional nano-walls in as-spun state. Moreover, XRD peaks shift of  $\alpha$ -Al and the absence of XRD peaks corresponding to Al-Mg phases refer to the formation of supersaturated solid solution of Mg in  $\alpha$ -Al. Ultimate tensile strength of the as spun ribbons was as high as 300 MPa. This improvement in the microstructure and tensile properties may be attributed to the supersaturated solid solution of Mg in  $\alpha$ -Al and the formation of  $\text{Al}_4\text{C}_3$  two dimensional nano-walls in melt spun state.

© 2016 Trade Science Inc. - INDIA

### KEYWORDS

Melt spinning;  
Al-Mg alloys;  
Aluminum carbide;  
Aluminum matrix composite;  
X-ray diffraction;  
Scanning electron microscopy;  
Thermal analysis.

### INTRODUCTION

Melt spinning technique is a rapid quenching process with cooling rates higher than  $10^3$  K/s that allow the preparation of alloys with remarkable properties; i.e. reduction in grain sizes, extended solid solution ranges, reduced levels of segregation and in some cases the formation of metastable crystalline and amorphous phases<sup>[1-2]</sup>. Silicon carbide particles reinforced metal–matrix composites (MMCs) have been considered as excellent candidates to be applied as structural materials in the aeronautic–aerospace transport, the automotive industry,

etc.<sup>[3,4]</sup>. Al–Mg alloy is considered as one of the most widely used structural materials because of its remarkable properties, such as low density, high specific strength and so on<sup>[5]</sup>. However, its properties may be greatly influenced by the formation of different alloy phases. For instance, the  $\text{Al}_{12}\text{Mg}_{17}$  phase on the grain boundary will result in poor creep strength<sup>[6]</sup>. Although the equilibrium solid solubility of Mg in Al is about 1 wt.% at room temperature<sup>[7,8]</sup>, extended solid solubility of Mg in Al can be achieved by rapid solidification. It is reported that the solid solubility of Mg in  $\alpha$ -Al can be extended far beyond the equilibrium

## Full Paper

Concentrations up to about 34.6 mass% by rapid quenching<sup>[9]</sup>. It is well known that the SiC reinforcements tend to react with the active molten Al leading to the formation of  $\text{Al}_4\text{C}_3$  and Si at the interface<sup>[10,11]</sup>. It is noted that the formation of  $\text{Al}_4\text{C}_3$  is beneficial to the enhancement of thermal conductivity to a certain degree<sup>[12]</sup>. Moreover, it is mentioned that  $\text{Al}_4\text{C}_3$  may be a potent nucleating substrate for primary Mg due to its excellent thermal stability and therefore, Mg-50%  $\text{Al}_4\text{C}_3$ -6%Ce master alloy addition could refine the microstructure of AZ91D alloy<sup>[13]</sup>. In the microstructure studies on carbon fiber/Al composites, it was mentioned that  $\text{Al}_4\text{C}_3$  is a very important interfacial reactant. Its formation and size could significantly affect the interface combination and the property of composites. Moreover, it was suggested that the formation of  $\text{Al}_4\text{C}_3$  was controlled by the activity of Al element and it explained the formation mechanism of  $\text{Al}_4\text{C}_3$  by thermodynamic<sup>[14,15]</sup>. Here we report the synthesis of  $\text{Al}_4\text{C}_3$  nano-sheets with nano-wall which were observed at the interface of SiC/Al-Mg composites which fabricated by melt spinning technique.

## EXPERIMENTAL

### 2-1 materials preparation

A binary Al-10 wt.% Mg alloy was prepared from 99.8 wt.% pure Al, 99.75 wt.% pure Mg. The ingots were melting in a muffle furnace and SiC nanoparticles was incorporated to the molten Al-

Mg alloy using mechanical mixing method to prepare Al-10Mg-2SiC nanocomposite. The nanocomposite was poured into a graphite mold after the homogenization process to produce rods of 25mm in length and 4mm in diameter. Long uniform ribbons of thickness around 50  $\mu\text{m}$  and width 2mm were prepared by melt spinning technique. A stream of the molten alloy, at 900 °C, was ejected by argon gas at a gauge pressure of 1.5 bars from a silica tube with a 0.4mm orifice diameter. The melt jet fell on a copper disc of 18 cm diameter coated by chromium, rotating at 2950 rpm. The estimated cooling rate was about  $10^5 \text{ K/s}$ . The produced ribbons were fairly uniform. Deviations of 0.05% mm and 3  $\mu\text{m}$  in width and thickness were observed from the whole length of ribbons.

### Materials characterization

XRD patterns were performed using a 1390 Philips diffractometer with filtered Cu K $\alpha$  radiation at 40 kV and 20 mA. The X-ray samples were performed from a short length stuck on a glass slide using Vaseline. Microstructure characterizations were performed by scanning electron microscopy. SEM investigations were carried out in a JEOL JSM-T330 scanning electron microscope operated at 20 kV and linked with an energy dispersive spectrometry (EDS) attachment. The ribbons were observed for the wheel side surface using standard metallographic techniques. Optical mount specimens were prepared for SEM investigations

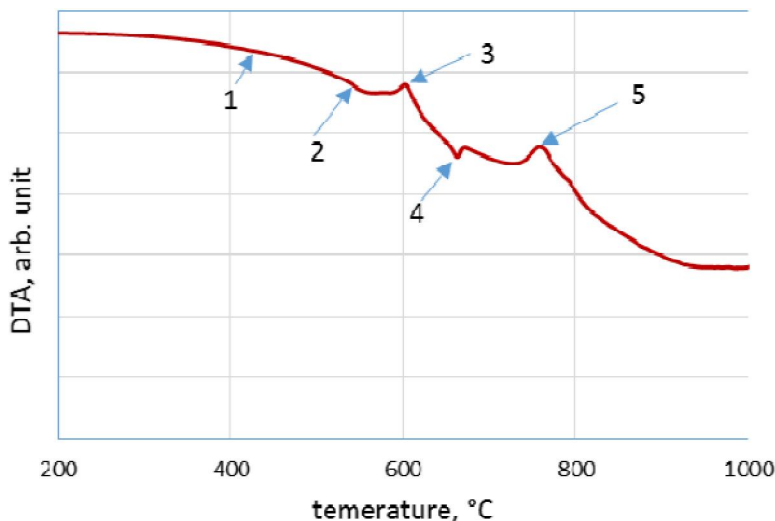


Figure 1 : DTA heating curves of SiC/Al-Mg as-spun composite heated at 10 °C/min

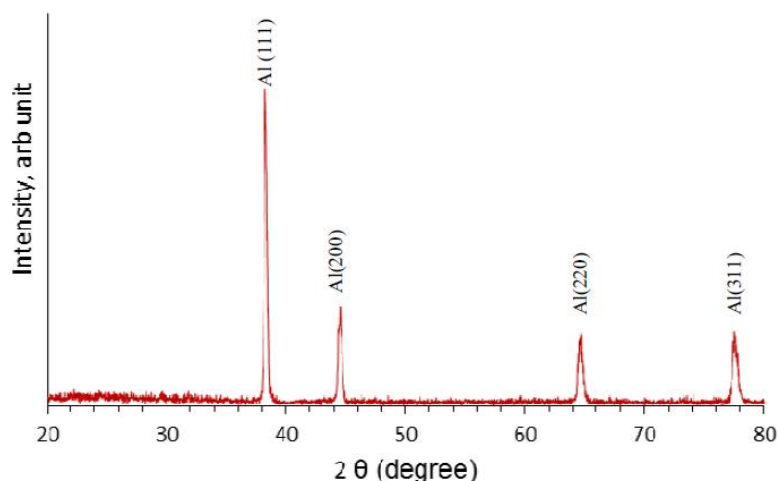


Figure 2 : XRD pattern of SiC/Al-Mg as-spun composite

TABLE 1 : Comparison of XRD peaks position of  $\alpha$ -Al in case of wheel side of SiC/Al-Mg as-spun composite ribbon and standard Al

2θ(degree)	Al(1 1 1)	Al(2 0 0)	Al(2 2 0)	Al(3 1 1)
Wheel side	38.2196	44.3842	64.6556	77.6079
Standard Al	38.473	44.739	65.135	78.229

followed by chemical etching in a 0.5% HF solution. The ribbons were tensile tested on an Instron machine. The test was performed on ribbons of gauge length 50 mm at room temperature and head speed of 3 mm min<sup>-1</sup>.

## RESULTS AND DISCUSSION

### DTA and X-ray diffraction analysis

Figure 1 shows DTA heating curve of SiC /Al-10Mg as-spun composite. According to the Al-Mg phase diagram and considering the supersaturated solid solution of Mg in  $\alpha$ -Al obtained during the rapid solidification process, one can interpret the obtained DTA signal. At temperature range of 350-520 °C, DTA signal decrease by increasing of the temperature that may be related to the relaxation of the supersaturated solid solution of  $\alpha$ -Al matrix. At higher temperature, the DTA signal increases forming the first exothermic peak around 602.2 °C which may related to a complete dissolution of Mg atoms from the  $\alpha$ -Al matrix. At temperature of 662.5 °C, an endothermic peak is formed which consistent with the melting point of  $\alpha$ -Al. It is reported that interfacial reaction between molten Al and SiC occurs only above 923 K (650 °C)<sup>[16]</sup>. Therefore, The second exo-

thermic peak which formed at 758.5 °C may be related to the decomposition of Al<sub>4</sub>C<sub>3</sub> phase.

Figure 2 shows XRD pattern obtained for the as-spun Al-10Mg-2SiC alloy. It can be seen that the main phase of the as-spun alloys is only  $\alpha$ -Al while Al<sub>12</sub>Mg<sub>17</sub> phase is not detected indicating that the rapid solidification results in an increase in the solubility of Mg in the Al matrix, and it is agreed with the high cooling rate during the melt-spun process which suggests that the solidification is primarily diffusionless and Mg is entrapped in the Al matrix. The supersaturated solubility of Mg in the Al matrix led to increase of the lattice parameter of  $\alpha$ -Al (up to 4.085519 nm instead of 4.05147 nm for casting pure Al), and finally resulted in diffraction peak shifts of the  $\alpha$ -Al to smaller 2θ direction. The XRD peak shifts of  $\alpha$ -Al for the AlMgSiC as-spun ribbon relative to the standard Al are listed in TABLE 1. This increase in lattice parameter of  $\alpha$ -Al has been reported from rapidly quenched alloys and mechanically milled alloys<sup>[17-19]</sup>. The average crystallite size and induced microstrain% of  $\alpha$ -Al are 99 nm and 0.137 respectively. The lattice parameter of  $\alpha$ -Al increases linearly with the Mg content as a solid solution in  $\alpha$ -Al. It is found that the lattice parameter of 0.4085519 is corresponding to about 10 wt%



## Full Paper

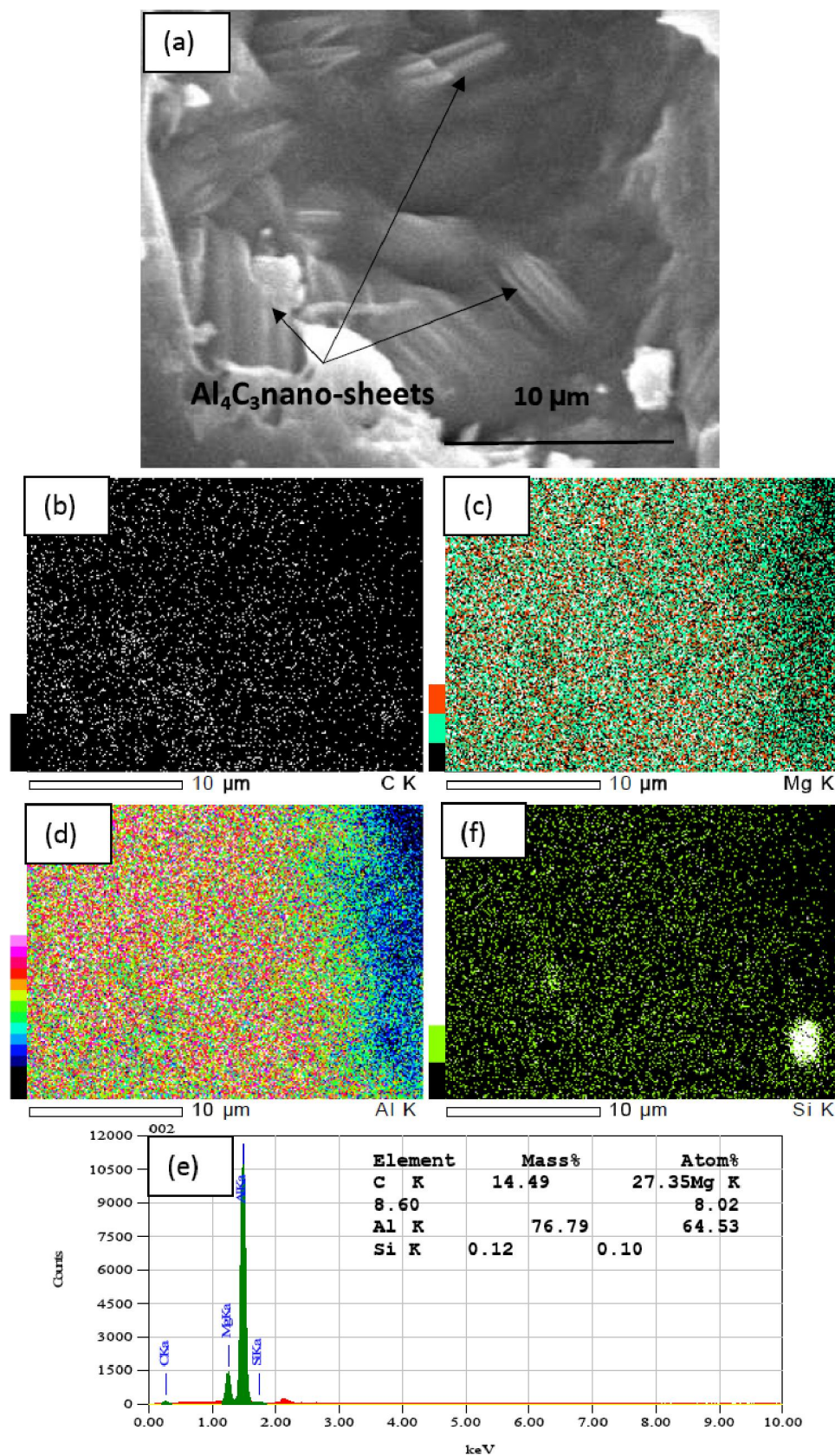
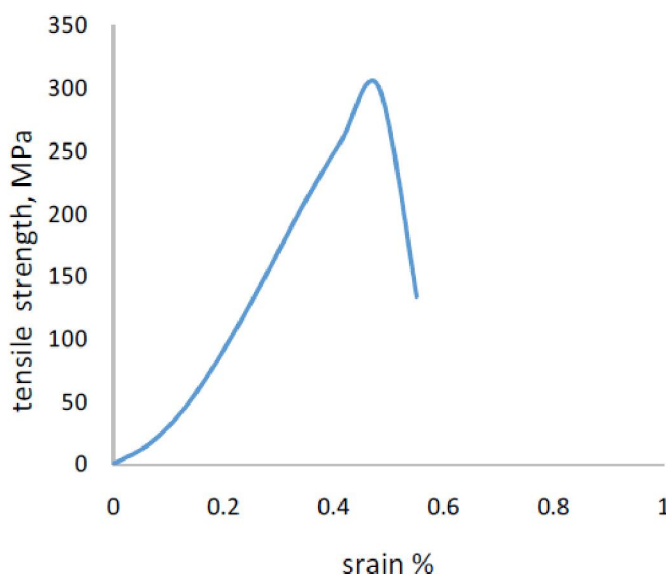


Figure 3 : SEM micrograph of SiC/Al-Mg as-spun composite (a); corresponding elemental maps of C (b), Mg (c), Al (d) and Si (e); corresponding EDS spectra of  $\text{Al}_4\text{C}_3$  phase (f).



**Figure 4 : Tensile test of as spun 2SiC/Al-10Mg nanocomposite with constant strain rate of 5 mm/min**

Mg as a solid solution in  $\alpha$ -Al at the wheel side of Al-10Mg-SiC ribbon alloy<sup>[20]</sup>. The peaks corresponding to  $\text{Al}_4\text{C}_3$  were ambiguous because the content of  $\text{Al}_4\text{C}_3$  was below the detection limit of XRD

### Scanning electron microscopy

The representative morphologies of the SiC/Al-Mg as-spun composite has been studied by scanning electron microscopy. Figure 3(a) shows the top-view image of a vertical nanowalls distributed uniformly in the SiC/Al-Mg as-spun composite. The corresponding elemental maps confirmed the existence of elements such as Al, C, Si and Mg as shown in Fig.3(b-e). Moreover, Figure 3(a) represents nano-sheets of bright lines that imply nanowalls with a vertical orientation and the dark areas indicate a concave surface. In addition, SEM image demonstrates that a typical nanowall has the morphology of an arcuate plate with a jagged edge which is smooth in the lateral plane and usually have a thickness of 100–200 nm but with random lengths and widths. EDX analysis confirmed that this nano-sheets are similar to  $\text{Al}_4\text{C}_3$  in composition as shown in Figure 3(f). The formation of  $\text{Al}_4\text{C}_3$  in nano-scale may interpret the absence of the corresponding XRD pattern.

### Tensile test

The present tensile test result of SiC/Al-Mg as spun composite clearly indicates that the strength increase to higher value (300 MPa) as compared to

Al-Mg matrix unreinforced alloy (190MPa)<sup>[21]</sup>. This improved tensile properties are proposed to be strongly determined by  $\alpha$ -Al supersaturated solid solution strengthening originated by Mg dissolving in  $\alpha$ -Al. In addition of the  $\text{Al}_4\text{C}_3$  nano-sheet which impede the movement of dislocations glide and climb, resulting in an upper ultimate strength.

### CONCLUSION

Al-10Mg-2SiC nanocomposite was successfully rapidly solidified by melt spinning technique. The microstructure showed excellent distribution of Mg, Si and C into Al matrix as deduced by SEM analysis. In addition, EDX analysis proved the formation of  $\text{Al}_4\text{C}_3$  nanosheet of two dimensional nano-walls in as-spun state as a result of chemical reaction of SiC with the molten Al. Moreover, XRD peaks shift of  $\alpha$ -Al and absence of Mg corresponding XRD pattern indicate to the formation of supersaturated solid solution of Mg in  $\alpha$ -Al. Ultimate tensile strength of the as spun ribbons was as high as 300 MPa. This improvement in the microstructure and tensile properties may be attributed to the supersaturated solid solution of Mg in  $\alpha$ -Al and the formation of  $\text{Al}_4\text{C}_3$  two dimensional nano-walls in melt spun state.

### ACKNOWLEDGEMENT

The author is grateful to both Taif university and

## Full Paper

National Research Center for providing financial support for this research.

### REFERENCES

- [1] F.V.Beaumont; The International Journal of Powder Metallurgy, **36(6)**, 41 (2000).
- [2] F.H.Samuel; Metallurgical Transactions, **17A**, 127 (1986).
- [3] J.Hashim; J.Mater.Process.Technol., **123**, 251 (2002).
- [4] P.Rohatgi; J.Minerals, **43**, 10 (1991).
- [5] A.K.Vasudevan, R.D.Doherty; Aluminum alloys – contemporary research and applications, Academic Press, New York, (1989).
- [6] A.Munitz, C.Cotler, A.Stern, G.Kohn; Mater.Sci.Eng., **302A**, 68 (2001).
- [7] T.B.Massalski; Binary alloy phase diagrams, (ASM International, Materials Park, OH, (1992).
- [8] N.Saunders; CALPHAD, **14**, 61 (1990).
- [9] H.L.Luo, C.C.Chao and P.Duwez; Trans.Metall.Soc.AIME, **230**, 1488 (1964).
- [10] R.Warren, C.H.Anderson; Composite, **15**, 101 (1984).
- [11] M.Gu, Z.Mei, Y.Jin, Z.Wu; Scripta.Mater., **40**, 985 (1999).
- [12] Q.U.Xuan-hui, Z.H.A.N.G Lin, W.U.Mao, R.E.N Shu-bin; Progress in Natural Science: Materials International, **21**, 189 (2011).
- [13] H.Hui, L.Cheng, M.Huaming, L.Shengfa, W.Shuoli, Y.Xinxing; Rare Metal Materials and Engineering, **42**, (2013).
- [14] S.H.Li, C.G.Chao; Metall.Mater.Trans., **35A**, 2153 (2004).
- [15] X.Wang, D.M.Jiang, G.H.Wu, B.Li, P.Z.Li; Mater.Sci.Eng., **497A**, 31 (2008).
- [16] S.Valdez, B.Campillo, R.Pérez, L.Martínez, A.García H; Matt.Lett., **62**, 2632 (2008).
- [17] H.L.Luo, C.C.Chao, P.Duwez; Trans.Metall.Soc.AIME, **230**, 1488 (1964).
- [18] M.Schoenitz, E.L.Dreizin; J.Mater.Res., **18**, 1827 (2003).
- [19] S.Scudino, S.Sperling, M.Sakaliyska, C.Thomas, M.Feuerbacher, K.B.Kim, H.Ehrenberg; J.Eckert; Acta.Mater., **56**, 1136 (2008).
- [20] K.Kaneko, T.Hatai, T.Tokunaga, Z.Horita; Materials Transactions, **50**, 76 (2009).
- [21] M.Emamy, A.R.Daman, R.Taghiabadi, M.Mahmudi; International Journal of Cast Metals Research, **17**, 17 (2004).